Synthesis and Photochemical Studies on Gallium and Indium Complexes of DTPA-PEG3-ArN3 for Radiolabeling Antibodies

Gut, Melanie ; Holland, Jason P

Abstract: Photochemistry is a rich source of inspiration for developing alternative methods to functionalize proteins with drug molecules, fluorophores, and radioactive probes. Here, we report the synthesis and photochemical reactivity of a modified diethylenediamine pentaacetic acid chelate that was derivatized with a light-responsive aryl azide group (DTPA-PEG3-ArN3, compound 1). The corresponding nonradioactive and radioactive nat/68Ga3+ and nat/111In3+ complexes of DTPA-PEG3-ArN3 were synthesized and their physical and photochemical properties were studied to evaluate the potential of employing this ligand system in the photochemical synthesis of radiolabeled antibodies. Photodegradation kinetics revealed that irradiation with ultraviolet light (365 nm) induced rapid photoactivation of compound 1 and the metal complexes nat/68Ga-1– and nat/111In-1–. Light-induced reactions were complete in <100 s, with measured first-order rate constants of 0.078 ± 0.045 s–1, 0.093 ± 0.009 s–1, and 0.117 ± 0.054 s–1 (n = 2, per species) for compound 1, natGa-1–, and natIn-1–, respectively. Photochemically induced bioconjugation reactions between DTPA-PEG3-ArN3 and the monoclonal antibody trastuzumab, as well as pre- and postconjugation 68Ga- and 111In-radiolabeling experiments, were performed using either a one-pot or two-step strategy. Both approaches yielded radiolabeled trastuzumab ([68Ga]GaDTPA-azepin-trastuzumab) with average radiochemical conversions of 3.9 ± 1.0% (n = 4, one-pot), and 10.0 ± 1.0% (n = 3, two-step). One-pot radiolabeling reactions with [111In]InCl3 produced the corresponding [111In]InDTPA-azepin-trastuzumab radiotracer in a similar radiochemical conversion of 5.4 ± 0.8% (n = 3). Radiochemical conversions for the desired bimolecular coupling between the chelate and the protein were comparatively low. This observation is likely caused by the high photoinduced reactivity of the compounds and subsequent competition with background reactions. Nevertheless, access to DTPA-PEG3-ArN3 increases the scope of photoradiochemical methods to include metal ions like In3+ that form complexes with higher coordination numbers.

DOI: https://doi.org/10.1021/acs.inorgchem.9b01802

Synthesis and Photochemical Studies on Gallium and Indium Complexes of DTPA-PEG_3-ArN_3 for Radiolabelling Antibodies

Melanie Gut and Jason P. Holland*

University of Zurich, Department of Chemistry, Winterthurerstrasse 190, CH-8057, Zurich, Switzerland

*** Corresponding Author:**

Prof. Dr Jason P. Holland

Tel: +41.44.63.53.990

E-mail: jason.holland@chem.uzh.ch

Website: www.hollandlab.org

First author:

Melanie Gut

Email: melanie.gut@chem.uzh.ch

Running Title: *Photoradiochemistry with DTPA-PEG_3-ArN_3*

Words (Main text): 4016

Abstract

Photochemistry is a rich source of inspiration for developing alternative methods to functionalise proteins with drug molecules, fluorophores and radioactive probes. Here, we report the synthesis and photochemical reactivity of a modified diethylenediamine pentaacetic acid chelate that was derivatised with a light-responsive aryl azide group (DTPA-PEG_3-ArN_3, compound **1**). The corresponding non-radioactive and radioactive $^{nat/68}Ga^{3+}$ and $^{nat/111}In^{3+}$ complexes of DTPA-PEG_3-ArN_3 were synthesised and their physical and photochemical properties were studied to evaluate the potential of employing this ligand system in the photochemical synthesis of radiolabelled antibodies. Photodegradation kinetics revealed that irradiated with ultraviolet light (365 nm) induced rapid photoactivation of compound **1**, and the metal complexes $^{nat/68}$Ga-**1**$^-$ and $^{nat/111}$In-**1**$^-$. Light-induced reactions were complete in < 100 s, with measured first-order rate constants of 0.078 ± 0.045 s^{-1}, 0.093 ± 0.009 s^{-1} and 0.117 ± 0.054 s^{-1} ($n = 2$ per species) for compound **1**, ^{nat}Ga-**1**$^-$ and ^{nat}In-**1**$^-$, respectively. Photochemically induced bioconjugation reactions between DTPA-PEG_3-ArN_3 and the monoclonal antibody trastuzumab, as well as pre- and post-conjugation ^{68}Ga- and ^{111}In-radiolabelling experiments were performed using either a one-pot or two-step strategy. Both approaches yielded radiolabelled trastuzumab ([^{68}Ga]GaDTPA-azepin-trastuzumab) with average radiochemical conversions of $3.9 \pm 1.0\%$ ($n = 4$, one-pot), and $10.0 \pm 1.0\%$ ($n = 3$, two-step). One-pot radiolabelling reactions with [^{111}In]$InCl_3$ produced the corresponding ([^{111}In]InDTPA-azepin-trastuzumab radiotracer in a similar radiochemical conversion of $5.4 \pm 0.8\%$ ($n = 3$). Radiochemical conversions for the desired bimolecular coupling between the chelate and the protein were comparatively low. This observation is likely caused by the high photo-induced reactivity of the compounds, and subsequent competition with background reactions.

Nevertheless, access to DTPA-PEG_3-ArN_3 increases the scope of photoradiochemical methods to include metal ion like In^{3+} that form complexes with higher coordination numbers.

Keywords: photoradiochemistry, aryl azide, radiochemistry, antibodies, gallium-68, indium-111

Introduction

Antibody-based radiotracers are frequently used in Nuclear Medicine for positron-emission tomography (PET) imaging.[1–5] Such agents facilitate cancer diagnosis and can be used to monitor the effectiveness of chemotherapies. Selecting alternative radionuclides like ^{67}Ga and ^{111}In allows for the development of radioimmunotherapeutics (RITs).[6] Traditional bioconjugation methods that are used to modify antibodies and other biomolecules with radionuclides typically require multiple chemical steps. First, the biomolecule is purified to remove formulation components that can interfere with the chemistry, and then the chelate is conjugated to the protein *via* standard ligation methods (amide, thioester or maleimide thiol couplings to cysteines or lysines etc). In this two-step conjugation and radiolabelling approach, the conjugated intermediate must also be re-purified to remove unreacted chelate that can compromise the radiochemistry. Finally, the chelate-biomolecule conjugate is radiolabelled, re-purified and characterised before use *in vitro* or *in vivo*.[2–5,7,8]

Photoreactions were employed for bioconjugations.[9–11] However, there are only a few examples whereby photochemical conjugation was used in the synthesis of radiotracers.[12–17, 18-21] Recently, our group demonstrated that photoradiochemical conjugation methods using different photoactive macrocyclic and acyclic chelates suitable for complexation of gallium, copper or zirconium radionuclides can be successfully coupled to proteins *via* light-induced activation of an

aryl azide (ArN_3) group. Photoradiosynthesis was completed in ~10 min starting directly from fully formulated antibody solutions (avoiding pre-purification and buffer exchange of the antibody), in high radiochemical yields (up to ~75%), and without compromising the structural integrity or biological viability of the protein.[18–21] However, a current restriction is that all reported photoactive chelates are limited to a maximum of 6 donor atoms which makes them unsuitable for coordination chemistry using larger metal ions like In^{3+} that preferentially form complexes with higher coordination numbers.

Diethylenetriaminepentaacetic acid (DTPA) is a high affinity binder of several metal cations. It bears three tertiary amines, and five sterically unconstrained carboxylic acids which can coordinate metal ions or be used as functionalisation handles.[22,23] The DTPA chelate has been wildly used in nuclear chemistry due to the fact that it forms stable coordination compounds with various metal ions including, indium[24] (formation constant log β = 29.0 – 29.5), yttrium[24] (log β = 21.2 – 22.5), gallium[24] (log β = 25.5) and lanthanides like gadolinium[25] (log β = 22.46).[22,23,26–32] Several ^{111}In-radiolabelled antibodies that incorporated the DTPA chelate have received clinical approval for SPECT imaging. These include ^{111}In-satumomab pendetide for the diagnosis of colorectal and ovarian carcinomas[33], and ^{111}In-capromab pendetide for prostate cancer therapy.[34–36]

Here, we attached the photoactive aryl azide group to DTPA *via* the use of a trimeric polyethylene glycol (PEG_3) spacer to yield DTPA-PEG_3-ArN_3 (compound **1**). This photoactive DTPA derivative broadens the metal ion scope of photo-induced conjugation reactions as it readily forms complexes with Gd^{3+} ions for developing magnetic resonance imaging (MRI) agents, $^{67}Ga^{3+}$ or $^{111}In^{3+}$ ions for combination with single-photon emission computed tomography and RIT, and $^{68}Ga^{3+}$ ions for positron emission tomography (PET). The photochemical properties and activation

kinetics of DTPA-PEG_3-ArN_3, and the corresponding non-radioactive and radioactive gallium and indium complexes, were studied by irradiation with 365 nm light in water. Moreover, the efficiency of light-induced conjugation of the photoactive chelate and the radioactive ^{68}Ga- and ^{111}In-complexes with trastuzumab (anti-human epidermal growth factor receptor 2, human IgG_1, Genentech, CA) was studied using both a traditional two-step, and a new one-pot photoradiochemical process.

Methods and Materials

Full experimental details and characterisation data for all synthetic steps, radiochemistry and photochemical reactions are presented in the Electronic Supporting Information.

Results and Discussion

Synthesis of DTPA-PEG_3-ArN_3 and the $^{nat}Ga^{3+}$ and $^{nat}In^{3+}$ complexes

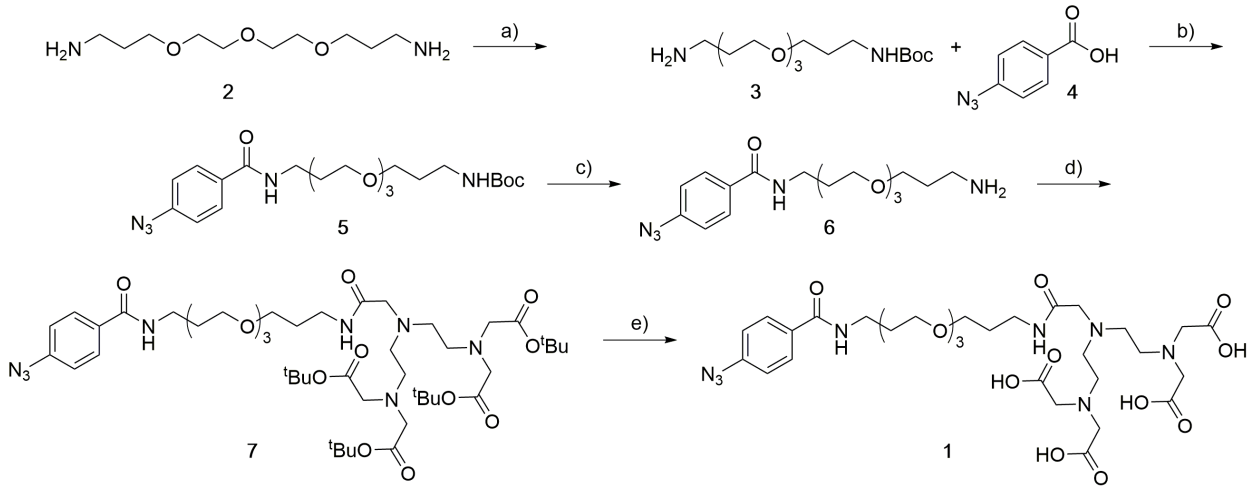

Scheme 1. Synthesis of DTPA-PEG_3-ArN_3 (**1**): a) Boc_2O, CH_2Cl_2, 0 °C to rt; b) HATU, DIPEA, DMF, rt; c) TFA, CH_2Cl_2, rt; d) DTPA-$(tBu)_4$ ester, HATU, DIPEA, DMF, rt; e) TFA, rt

DTPA-PEG_3-ArN_3 (compound **1**) was synthesised in five linear steps (Scheme 1) using chemical transformations starting from the key reagents 4-azidobenzoic acid, 3,3'-((oxy*bis*(ethane-2,1-diyl))*bis*(oxy))*bis*(propan-1-amine), and 3,6,9-*tris*(2-(tert-butoxy)-2-oxoethyl)-13,13-dimethyl-11-oxo-12-oxa-3,6,9-triazatetradecan-1-oic acid (also known as DTPA-$(tBu)_4$ ester). Synthesis and full characterisation of the pegylated aryl azide amine (compound **6**) was reported previously.[18] Compound **6** was coupled to the DTPA-$(tBu)_4$ ester using HATU chemistry to give the protected intermediate (**7**) which was deprotected without isolation using trifluoroacetic acid to afford compound **1** (DTPA-PEG_3-ArN_3) in an overall yield of 21%. Compound **1** was characterised by reverse-phase high-performance liquid chromatography (HPLC), high-resolution electrospray ionisation mass spectrometry (HR-ESI-MS), ^{1}H- and ^{13}C-NMR spectroscopy, and electronic absorption spectroscopy (Figures S1-S4).

After isolation and characterisation of compound **1**, the corresponding $^{nat}Ga^{3+}$ and $^{nat}In^{3+}$ complexes were prepared and characterised by HPLC, HR-ESI-MS, and electronic absorption spectroscopy (Figures S5-S8).

Photochemical activation kinetics

The photochemical properties of compound **1**, Ga-**1**$^-$ and In-**1**$^-$ were analysed by irradiating aqueous solutions with an ultraviolet, light emitting diode (LED) source with peak emission intensity at 364.5 nm (power output ~92 mW, with a full-width at half maximum of 9.1 nm). Aliquots of the irradiated solutions were analysed at different time points by HPLC. The three compounds showed higher photoreactivity than previously reported photoactive derivatives of *aza*-macrocycles and acyclic desferrioxamine B (DFO) or HBED-CC chelates bearing ArN_3 groups.[18–21] Kinetic studies revealed that compound **1**, Ga-**1**$^-$ and In-**1**$^-$ undergo rapid photo-

induced degradation with pseudo-first-order rate constants of 0.078 ± 0.045 s^{-1}, 0.093 ± 0.009 s^{-1}, 0.117 ± 0.054 s^{-1} (n = 2 independent replicated per species), respectively (Figure 1). Under the irradiation conditions employed, the formation of one major product peak was observed for each compound. Mass spectrometry analysis of the irradiated species indicated the formation of the corresponding water adducts (Figures S9-S12).

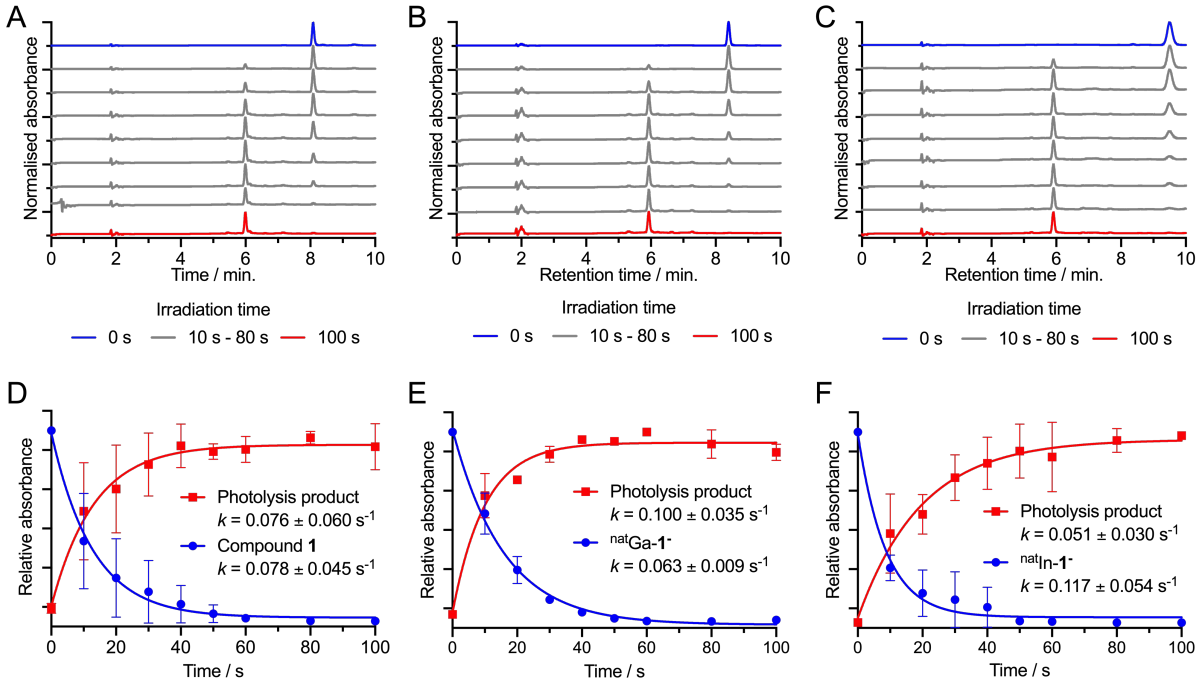

Figure 1. Photochemical activation kinetics showing the changes in the HPLC chromatograms (panels A – C), and the corresponding normalised integration of the peak intensities for starting material and major product for compound **1**, ^{nat}Ga-**1**$^{-}$ and ^{nat}In-**1**$^{-}$, respectively (panels D – F).

Radiosynthesis and photochemical activity of [^{68}Ga]GaDTPA-PEG$_3$-ArN$_3$ (^{68}Ga-**1**$^{-}$) and [^{111}In]InDTPA-PEG$_3$-ArN$_3$ (^{111}In-**1**$^{-}$)

After characterising the non-radioactive species, ^{68}Ga- and ^{111}In-radiolabelling and photoradiochemical activation experiments were performed (Figure 2). The radiolabelled ^{68}Ga-**1**$^{-}$

species was prepared by reacting compound **1** with an aliquot of [^{68}Ga][Ga(H_2O)$_6$]Cl_3(aq.) obtained from elution of a ^{68}Ge/^{68}Ga-generator with HCl (0.1 M) using standard radiochemical methods. ^{68}Ga-radiolabelling experiments were performed in acetate buffer (0.25 M, pH 4.4) at room temperature.

The radiolabelled ^{111}In-**1**$^{-}$ species was prepared by reacting compound **1** with an aliquot of [^{111}In][$InCl_3$(aq.) dissolved in HCl (0.1 M) (Curium Pharma, Paris, France) using standard radiochemical methods. ^{111}In-radiolabelling experiments were performed in acetate buffer (0.25 M, pH 4.4) at room temperature.

A comparison of the electronic absorption (λ = 254 nm) and radioactive chromatograms revealed that metal ion complexation gave a slight increase in retention on reverse-phase HPLC. The identity of the single radioactive peak obtained in the ^{68}Ga- and ^{111}In-radiolabelling reactions (Figure 2 (panel A: Ga; panel B: In), red traces) was confirmed by comparison of retention times and by standard co-elution (spike) methods using the authentic samples of ^{nat}Ga-**1**$^{-}$ (Figure 2 A, blue trace) and ^{nat}In-**1**$^{-}$ (Figure 2B, blue trace). Upon irradiation, photoactivation of both the Ga-**1**$^{-}$ (Figure 2A, green and orange traces) and In-**1**$^{-}$ (Figure 2B, green and orange traces) complexes occurred with complete loss of the peak associated with the starting complexes and formation of several new species (with one major product, *vide supra*) that eluted at shorter retention times. The experimental chromatograms are consistent with the photochemical activation kinetics and also with the proposed mechanism which primarily leads to the formation more polar intermediates and by-products.[37] Overall, these radiolabelling experiments confirmed that the compound **1** could be radiolabelled efficiently with two different radionuclides, and that photoactivation chemistry of the radioactive $^{nat/68}$Ga-**1**$^{-}$ and $^{nat/111}$In-**1**$^{-}$ complexes was equivalent at the different molar extents of the non-radioactive and radioactive reactions.

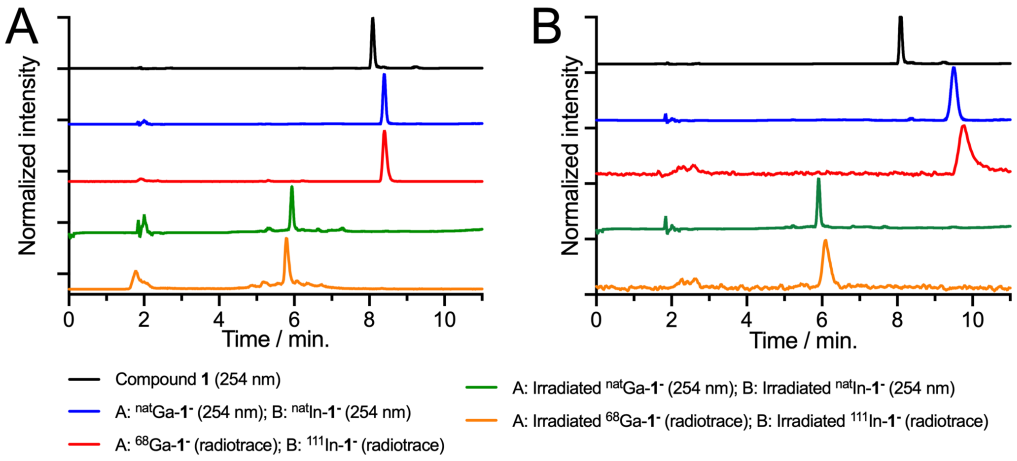

Figure 2. Normalised high-performance liquid chromatography (HPLC) data showing, a single peak for the elution of compound **1** (black), and single peaks observed for non-radioactive complex ^{nat}Ga-**1**$^{-}$ (A, blue) and ^{nat}In-**1**$^{-}$ (B, blue), co-elution of the radioactive species ^{68}Ga-**1**$^{-}$ (A, red) and ^{111}In-**1**$^{-}$ (B, red) confirming chemical identity, and the electronic absorption (254 nm) and radiochromatograms obtained after irradiating (365 nm, 10 min., 23 ^{o}C) ^{nat}Ga-**1**$^{-}$ (A, green) and ^{nat}In-**1**$^{-}$ (B, green), or ^{68}Ga-**1**$^{-}$ (orange) and ^{111}In-**1**$^{-}$ (B, orange).

Photochemical conjugation of DTPA-PEG$_3$-ArN$_3$ to trastuzumab

One-pot approach For our intended purpose of functionalising proteins with drugs, chelates or radioactive complexes, increased photochemical reactivity is desirable, but only if it does not compromise the efficiency of the desired bimolecular conjugation. Detailed experimental, spectrometric and computational work on the mechanism of photochemical activation, rearrangement to a ketenimine intermediate, and bimolecular nucleophilic attack by primary amines has been reported.[18–21] Extreme reactivity of the photo-induced intermediates is one of the numerous attractive features of utilising photochemistry to label antibodies but conversely it is also one of the main challenges. Specifically, after UV irradiation induces the loss of N_2(g) from ArN_3 to give an open-shell singlet nitrene, experimental conditions must be carefully controlled to

ensure that the reactivity of the electrophilic intermediates favours bimolecular coupling with an amine or carboxylate residue on the protein over non-productive intramolecular cyclisation or quenching by the background solvent (water).

Photochemical conjugation and radiolabelling experiments were performed to investigate the efficiency of light-induced functionalisation of trastuzumab using either a recently introduced one-pot or conventional two-step approach (Scheme 2).

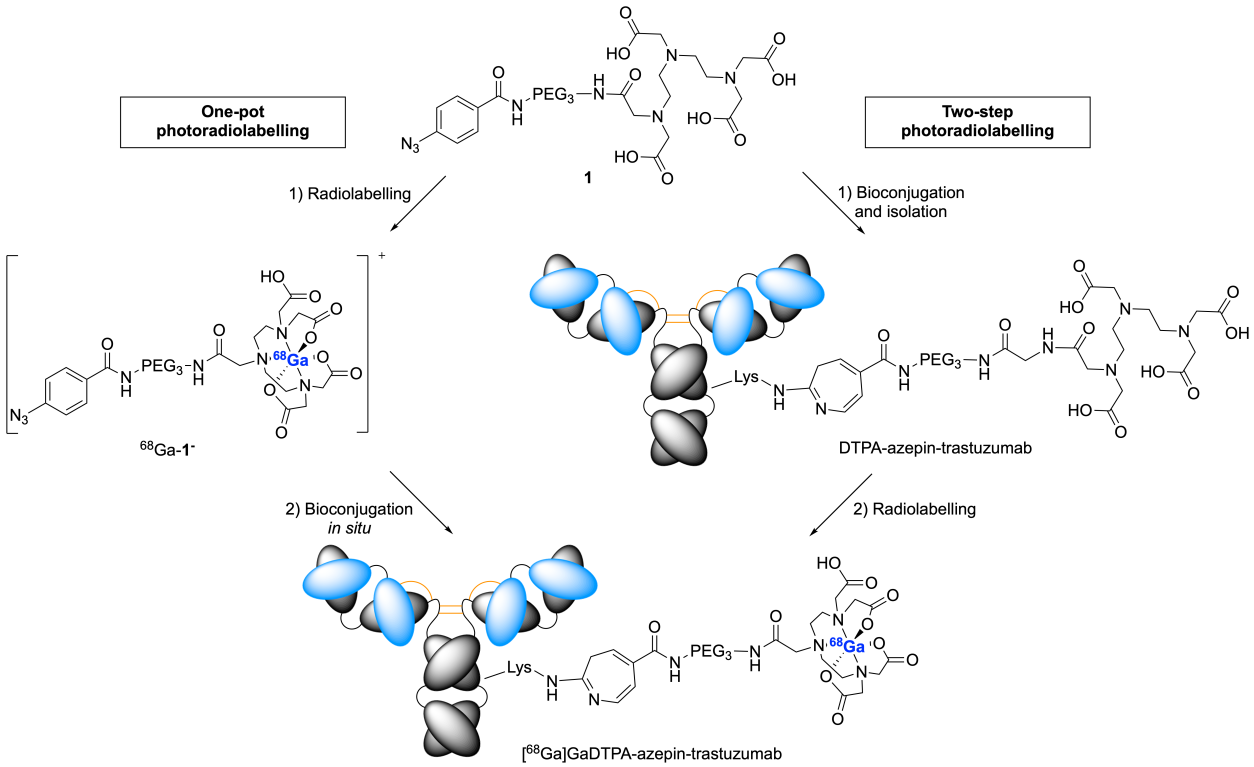

Scheme 2. Overview of the one-pot (left) and two-step (right) routes for photochemical conjugation and ^{68}Ga-radiolabelling of trastuzumab with DTPA-PEG$_3$-ArN$_3$. Note. An equivalent approach can be taken using ^{111}In.

All photochemical conjugation reactions were performed by irradiating reaction mixtures for 15 min. at 23 ^{o}C to ensure complete light-induced activation of the starting materials. Typically, an initial chelate-to-antibody mole ratio of 10:1 was used which was selected based on our prior

experience with ^{68}Ga-radiolabelled macrocyclic chelates.[18,19] In the one-pot approach, DTPA-PEG_3-ArN_3 (**1**) was dissolved in water, the pH was adjusted to ~4 – 4.5 using sodium acetate buffer, and then an appropriate aliquot of ^{68}Ga-chloride (with the activity formerly present as solvated $[^{68}Ga][Ga(H_2O)_6]^{3+}$, $[^{68}Ga][Ga(H_2O)_5(OH)]^{2+}$ or $[^{68}Ga][Ga(H_2O)_4(OH)_2]^{+}$ ions) or ^{111}In-chloride was added. The pH of the reaction was adjusted *in situ* to pH 7.7 – 8.3 using Na_2CO_3, after adding the radioactivity but before the addition of the antibody. Subsequently, the reaction mixtures were exposed to UV light. Aliquots of the crude reaction mixture were retained for further analysis, and a fraction was purified *via* standard spin-column centrifugation and solid-phase PD-10 size-exclusion chromatography (SEC) methods. All samples and appropriate controls were analysed by instant thin layer radiochromatography (radio-iTLC), analytical SEC PD-10 methods, and SEC radiochromatography. Data for the one-pot radiochemistry using ^{68}Ga are presented in Figure 3 and equivalent data using ^{111}In are given in Figure 4).

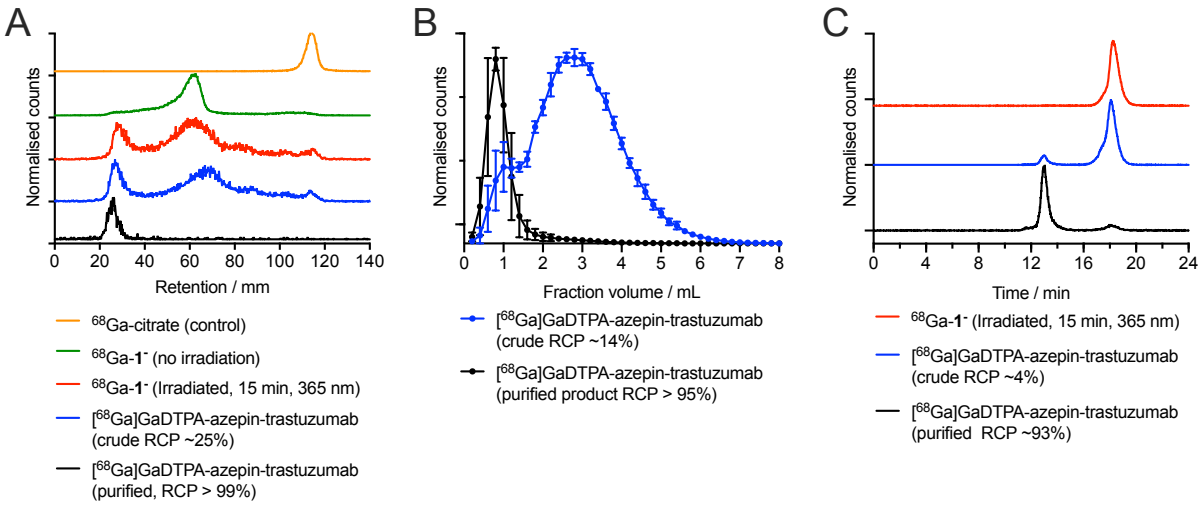

Figure 3. Analytical radiochemical data for the one-pot photoradiosynthesis of [^{68}Ga]GaDTPA-azepin-trastuzumab. (A) Radio-iTLC data showing the migration on silica gel strips for 'free' $^{68}Ga^{3+}$ ions (present as ^{68}Ga-citrate; orange control), ^{68}Ga-**1**$^{-}$ before irradiation (green), the mixture of ^{68}Ga-**1**$^{-}$ after irradiation in the absence of protein (red), and the crude (blue) and purified (black) [^{68}Ga]GaDTPA-azepin-trastuzumab species formed after irradiation in the

presence of the antibody. (B) PD-10 size-exclusion elution profiles showing the analysis of the crude (blue) and purified (black) [^{68}Ga]GaDTPA-azepin-trastuzumab species. (C) SEC radiochromatography data showing the elution profiles of ^{68}Ga-**1**$^{-}$ after irradiation in the absence of protein (red), the crude (blue) and purified (black) [^{68}Ga]GaDTPA-azepin-trastuzumab species.

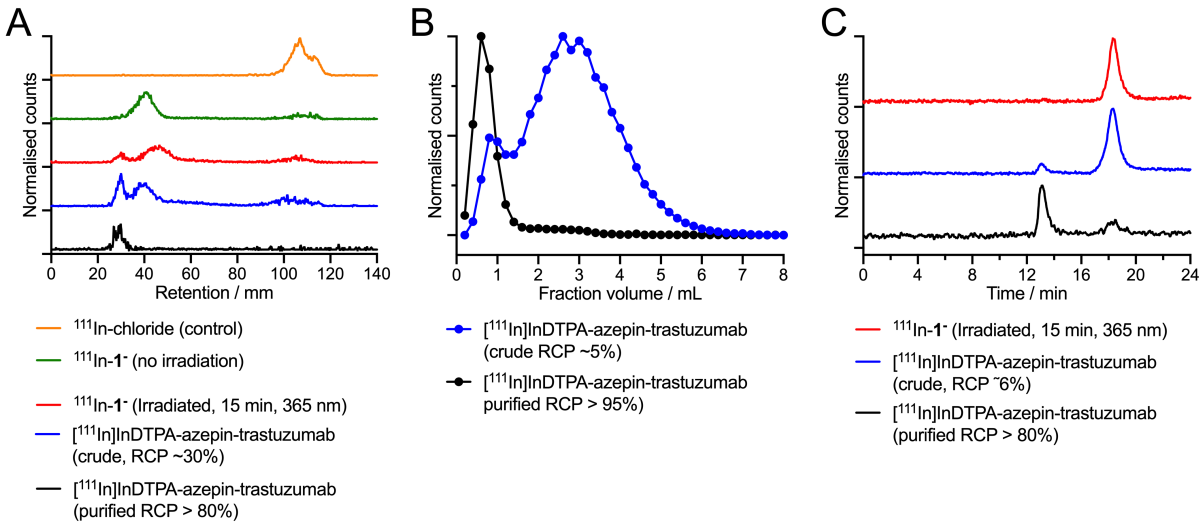

Figure 4. Analytical radiochemical data for the one-pot photoradiosynthesis of [^{111}In]InDTPA-azepin-trastuzumab. (A) Radio-iTLC data showing the migration on silica gel strips for 'free' ^{111}In^{3+} ions (present as ^{111}In-chloride; orange control), ^{111}In-**1**$^{-}$ before irradiation (green), the mixture of ^{111}In-**1**$^{-}$ after irradiation in the absence of protein (red), and the crude (blue) and purified (black) [^{111}In]InDTPA-azepin-trastuzumab species formed after irradiation in the presence of the antibody. (B) PD-10 size-exclusion elution profiles showing the analysis of the crude (blue) and purified (black) [^{11}1In]InDTPA-azepin-trastuzumab species. (C) SEC radiochromatography data showing the elution profiles of ^{111}In-**1**$^{-}$ after irradiation in the absence of protein (red), the crude (blue) and purified (black) [^{111}In]InDTPA-azepin-trastuzumab species.

Under the radio-iTLC conditions used (0.2 M sodium citrate, pH4.5) uncomplexed 'free' ^{68}Ga^{3+} and ^{111}In^{3+}species reacted with citrate and migrated to the solvent front (R_f = 1.0; Figures 3A and 4A, orange trace). The ^{68}Ga-**1**$^{-}$ and ^{111}In-**1**$^{-}$ migrated on the silica gel strips giving a broad

peak from approximately R_f = 0.25 – 0.60 and 0.15 – 0.35 (Figures 3A and 4A, green trace), respectively. Irradiation in the presence of the antibody led to retention of a fraction of the activity at the baseline (R_f = 0.0) which is indicative of radiolabelled protein as shown for the crude (Figures 3A and 4A, blue trace) and purified (Figures 3A and 4A, black trace) ^{68}Ga- and ^{111}In-DTPA-azepin-trastuzumab product. However, irradiation of the ^{68}Ga-**1**$^{-}$ and ^{111}In-**1**$^{-}$ also gave an increase in baseline activity due to the formation of more polar species which were retained on silica. Therefore, further confirmation that the radioactivity was bound to the protein, and accurate quantification of radiochemical conversions was obtained by analytical SEC PD-10 chromatography (Figures 3B and 4B) and by SEC radiochromatography (Figure 3C and 4C). For the one-pot reactions, an average radiochemical conversion of 3.9 ± 1.0% (n = 4; measured by SEC radiochromatography) and 5.4 ± 0.8% (n = 3; measured by SEC radiochromatography) was observed for either the ^{68}Ga or the ^{111}In complexes. Radiochemical purities >80% could only be obtained after extensive purification of the radiolabelled DTPA-azepin-trastuzumab. Given that an initial 10:1 chelate-to-mAb ratio was used, the estimated upper limit to the average number of ^{68}Ga or ^{111}In chelates bound per antibody was 0.39 ± 0.1 (n = 4) and 0.54 ± 0.1 (n = 3), respectively. We note that the actual chelate-to-mAb ratio in the final product is likely to be lower but accurate quantification is non-trivial due to the variations in molar activity and radiochemical purity of the ^{68}Ga and ^{111}In stock solutions.

Notably, the purification of ^{68}Ga- and ^{111}In-DTPA-azepin-trastuzumab from the large excess of radioactive small molecule species that also formed during the reaction was challenging. Crude mixtures were purified by multiple centrifugal filtration cycles using 30 kDa cut-off spin filters and also by preparative SEC PD-10. Purified product could be obtained after two cycles of PD-10 chromatography and centrifugal filtrations (4 times, 10 min.). The reason for the difficulties

encountered in purification is most likely caused by the low radiochemical conversion which makes it challenging to isolate the radioactive protein from the impurities (about 90%). Moreover, weak ion pair association of the anionic ^{68}Ga-**1**$^{-}$ and ^{111}In-**1**$^{-}$ (and related by-products) with cation residues (for example, lysine side-chains) on the protein might increase the separation difficulties.

Two-step approach using ^{68}Ga: Given that comparatively low photochemical conjugation efficiencies were observed by using the one-pot procedure, we also investigated the efficiency of a conventional two-step approach. First, pre-purified trastuzumab (spin filtration, 30 kDa cut-off) was photochemically conjugated with DTPA-PEG$_3$-ArN$_3$ using an initial 5:1 or 10:1 chelate-to-mAb ratio. The reactions were buffered with NaHCO$_3$ (1.0 M) to a pH between 7.9 – 8.3. The crude reaction mixtures were purified by preparative PD-10-SEC eluting with PBS. Prior to analysis, samples were concentrated centrifugal filtration. Aliquots of the crude and purified reaction mixtures were radiolabelled with ^{68}Ga^{3+} ions to measure the crude radiochemical purity (RCP) of [^{68}Ga]GaDTPA-azepin-trastuzumab. Radio-iTLC, PD-10 and SEC radiochromatography data are presented in Figure 5.

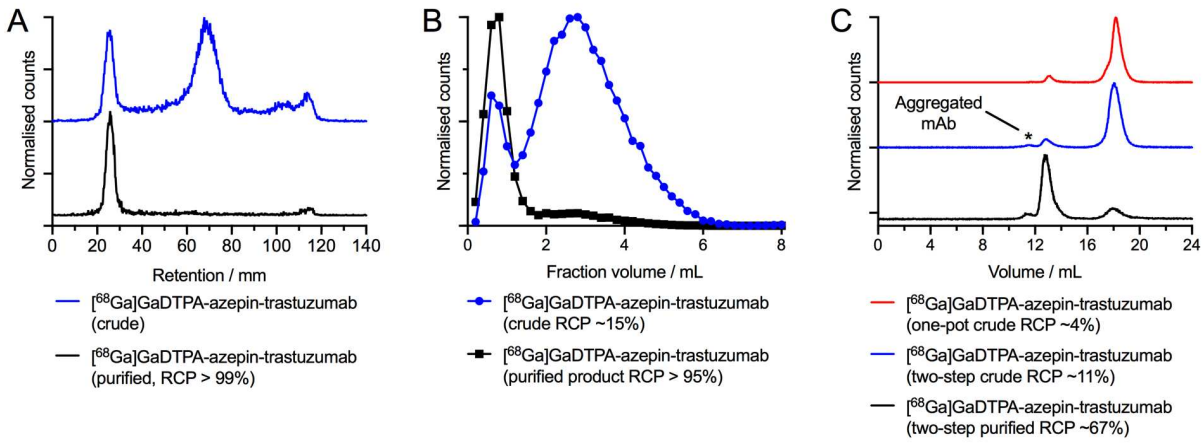

Figure 5. Analytical radiochemical data for the *two-step* photochemical conjugation and subsequent radiolabelling to form [^{68}Ga]GaDTPA-azepin-trastuzumab. (A) Radio-iTLC data showing the crude (blue) and purified (black)

[^{68}Ga]GaDTPA-azepin-trastuzumab species formed after irradiation in the presence of the antibody. (B) PD-10 size-exclusion elution profiles showing the analysis of the crude (blue) and purified (black) [^{68}Ga]GaDTPA-azepin-trastuzumab species. (C) SEC radiochromatography data showing crude elution profile [^{68}Ga]GaDTPA-azepin-trastuzumab after the one-pot synthesis (red) and equivalent data for the crude (blue) and purified (black) [^{68}Ga]GaDTPA-azepin-trastuzumab species produced *via* the two-step approach.

The average radiochemical conversion obtained *via* the two-step process (with an initial chelate-to-mAb ratio of 5:1) was 10.0 ± 1.0%, (n = 3). Increasing the chelate-to-mAb ratio to 10:1 showed only a minor increase in conversion to 12.8%. If one compares these results with the one-pot reactions with the same chelate-to-mAb ratio (10:1) but a lower protein concentration (53.8 vs. 89 μM, Table S1, Figure S13) these measured radiochemical conversions support the assumption of a first-order reaction with respect to the protein concentration. Since lower chelate-to-mAb ratios are preferred for antibody functionalisation due to the expense of the reagents, higher ratios were not investigated. Notably, the two-step process led to a higher fraction of aggregated / dimerised antibody in the final product (highlighted by the asterisk in Figure 5C, black trace) when compared to the one-pot reactions with either ^{68}Ga (Figure 3C, black trace) or ^{111}In (Figure 4C, black trace). In spite of the lower radiochemical conversion obtained *via* the one-pot method, reducing the fraction of aggregated protein is a crucial factor in optimising the pharmacokinetics and radiation dosimetry of radiolabelled antibodies *in vivo*.[20,34]

Overall, the experimental data confirm that photoactive DTPA-PEG$_3$-ArN$_3$ is a viable tool for use in the photoradiosynthesis of functionalised antibodies for the production of diagnostic probes or radioimmunotherapeutics.

Optimisation of the one-pot photochemical conjugation process

To investigate the concentration dependency of the photochemical conjugation reaction, different protein concentrations were evaluated in conjugation with the one-pot process. The conjugation with ^{111}In-**1**$^{-}$ showed a linear dependency of the conversion with respect to the protein concentration (Table S1 and Figure S13). At the lowest protein concentration of 19.7 μM only a very low RCY of 3.1 ± 0.1% (*n* = 2; Table S1 condition A) was obtained. Increasing the concentration to 39 μM increased the RCY to 5.4 ± 0.8% (*n* = 3; Figure S13 entry 2). At higher protein concentrations of 53 and 83 μM, radiochemical conversions of 6.9 ± 0.8% (*n* = 2; Table S2 condition B and Figure S13 entry 4) and 8.5 ± 1.8% (*n* = 2; Table S1 condition C and Figure S13 entry 6), respectively, were observed (Table S1). One-pot reactions with the ^{68}Ga-**1**$^{-}$ complex show a similar behaviour with an increase in RCY from 3.9 ± 1.0% (*n* = 4; Figure S13 entry 3) to 8.9% (*n* = 1; Figure S13 entry 5) when the mAb concentration was increased from 38 to 54 μM, respectively (Table S1, Figure S13).

These results provide further evidence to suggest that the photochemically induced conjugation reaction is first-order with respect to the protein concentration – as required due to the bimolecular nature of the coupling process. These data also indicate that, given the conditions employed, the product ratio between radiolabelled mAb and other photolysis by-products is likely under kinetic control. Full optimisation of the reaction conditions, and extensive kinetic experiments are beyond the scope of the current work but our experiments strongly suggest that a detailed understanding of the radiochemical kinetics will facilitate improvements in the efficiency of our photoradiosynthetic process.[38]

A comparison of the radiochemical conversions from the reaction of various ^{68}Ga-*aza*-macrocyclic complexes, ^{89}Zr-radiolabelled DFO-ArN_3, and ^{68}Ga-**1**$^{-}$ and ^{111}In-**1**$^{-}$ with pre-purified trastuzumab is presented in Table 1. Under very similar reaction conditions to our previous work

using *aza*-macrocyclic complexes, DTPA-PEG_3-ArN_3 gave the lowest one-pot radiochemical conversion to radiolabelled trastuzumab. Precise reasons as to why the use of compound **1** gave lower radiochemical conversions remain unknown. However, given that one-pot reactions using ^{68}Ga-**1**$^-$ and ^{111}In-**1**$^-$ complexes showed similar radiochemical conversions (3.9 ± 1.0% and 5.4 ± 0.8%, respectively), it seems plausible that kinetics, in the form of parallel reactions between productive mAb functionalisation and background quenching, is the limiting factor. Another potential reasons for the low radiochemical conversion observed could be the increased photochemical activation kinetics of compound 1, $^{nat/68}$Ga-1$^-$ and $^{nat/111}$In-1$^-$ (Figure 1) compared with equivalent measurements using other ligand systems (Table 1). There is also the possibility that the initial photolysis products undergo further photoactivated transformations (secondary photolysis) which would complicate the process. Further synthetic, spectroscopic and kinetic experiments are underway to investigate structure-activity relationships in more detail and to elucidate the nature of the competing side reactions that currently impose empirical limits on the radiochemical conversion efficiency.[20]

Compound name	**Radionuclide ion**	**Chemical structure of the chelate**	**Radiochemical conversion (%) ± S.D. (number of replicates)** [a]	**Reference**
DTPA-PEG_3-ArN_3 (**1**)	$^{68}Ga^{3+}$ and ^{111}In	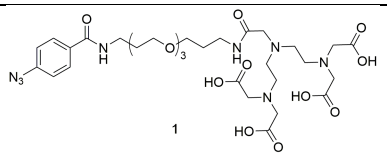 1	^{68}Ga: 3.9 ± 1.0% (n = 4) [b] ^{111}In: 5.4 ± 0.8% (n = 3) [b]	This work
NODAGA-PEG_3-ArN_3	$^{68}Ga^{3+}$	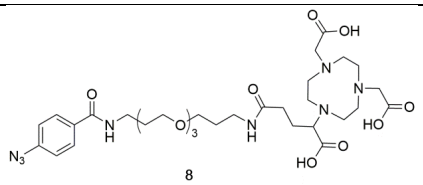 8	22.0 ± 3.5% (n = 3) [b]	Patra *et al*.[18]

NOTA-PEG$_3$-ArN$_3$	$^{68}Ga^{3+}$	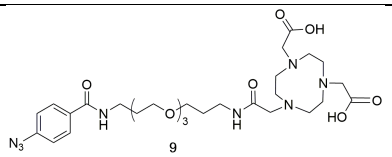 9	15.5 ± 1.5% (n = 3) [b]	Eichenberger *et al.*[19]
DOTA-PEG$_4$-ArN$_3$	$^{68}Ga^{3+}$	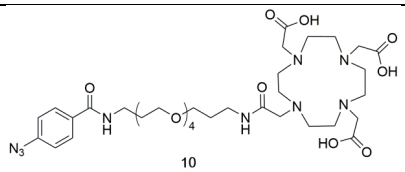 10	12.7 ± 3.2% (n = 3) [b]	Eichenberger *et al.*[19]
DOTAGA-PEG$_4$-ArN$_3$	$^{68}Ga^{3+}$	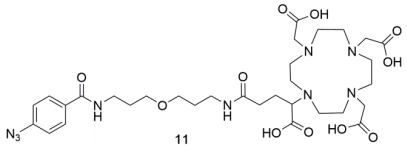 11	11.1 ± 0.2% (n = 3) [b]	Eichenberger *et al.*[19]
DFO-ArN$_3$	$^{89}Zr^{4+}$	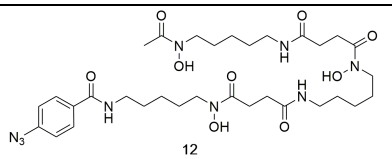 12	67% – 88% (n = 2) [b]	Patra *et al.*[20]
HBED-CC-PEG$_3$-ArN$_3$	$^{68}Ga^{3+}$	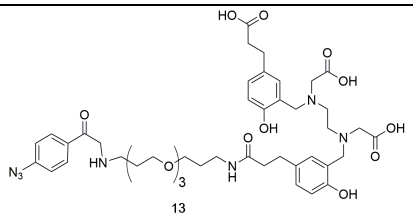 13	18.5 ± 0.5% (n = 2) [c]	Fay *et al.* [21]

Table 1. Comparison of the radiochemical conversions (as a percentage) obtained from the reaction of various ^{68}Ga- and ^{89}Zr-radiolabelled photoactive chelates with pre-purified antibodies.[18–21]

[a] Errors reported as one standard deviation from the mean. [b] One-pot photoradiolabelling using trastuzumab. [c] Two-step photoradiolabelling using onartuzumab.

Conclusions

The photoactive DTPA-PEG$_3$-ArN$_3$ (**1**) was synthesised, and characterised by using a range of chemical, spectroscopic, photochemical, kinetic and radiochemical methods. Non-radioactive experiments confirmed that the $^{nat}Ga^{3+}$ and $^{nat}In^{3+}$ complexes remained photochemically active with rapid photoactivation kinetics. ^{68}Ga- and ^{111}In-radiolabelling experiments confirmed that the ^{68}Ga-**1**$^-$ and ^{111}In-**1**$^-$ complexes could be produced rapidly using standard radiochemistry. The

radioactive complex exhibited equivalent photoactivity to the non-radioactive ^{nat}Ga and ^{nat}In complexes. Photochemical conjugation to pre-purified trastuzumab was successful and the radiolabelled ^{68}Ga- and ^{111}In-DTPA-azepin-trastuzumab product were obtained in comparatively low radiochemical conversions *via* either a one-pot or a classical two-step radiosynthetic procedure. Although the conjugation efficiency was lower than other reported photoactive complexes, access to DTPA-PEG_3-ArN_3 expands the potential chemical scope and utility of photo(radio)synthesis since the acyclic DTPA-chelate can accommodate larger metal ions (such as $^{111}In^{3+}$ or $^{nat}Gd^{3+}$) for future use in SPECT imaging, radioimmunotherapy or the development of targeted contrast agents for MRI.

Acknowledgements

JPH thanks the Swiss National Science Foundation (SNSF Professorship PP00P2_163683), the Swiss Cancer League (Krebsliga Schweiz; KLS-4257-08-2017), and the University of Zurich (UZH) for financial support. This project has received funding from the European Union's Horizon 2020 research and innovation programme / from the European Research Council under the Grant Agreement No 676904, ERC-StG-2015, NanoSCAN. We thank all members of the Radiochemistry and Imaging Science group at UZH for helpful discussions.

Associated Content

Supporting Information

The Supporting Information is available free of charge on the ACS Publications website at DOI:

Full details on the synthesis including NMR, HPLC, HR-MS and UV-Vis data can be found in Figures S1 – S8. Details on photochemistry and radiochemistry experiments can be found in the Supporting Information including HR-MS, SEC-HPLC and UV-Vis data (Figures S9 – S13, and Table S1).

References

(1) Boswell, C. A.; Brechbiel, M. W. Development of Radioimmunotherapeutic and Diagnostic Antibodies: An inside-out View. *Nucl. Med. Biol.* **2007**, *34* (7), 757–778. https://doi.org/10.1016/j.nucmedbio.2007.04.001.

(2) Zeglis, B. M.; Lewis, J. S. The Bioconjugation and Radiosynthesis of 89Zr-DFO-Labeled Antibodies. *J. Vis. Exp.* **2015**, *49* (7), 52521. https://doi.org/10.3791/52521.

(3) Zeglis, B. M.; Lewis, J. S. A Practical Guide to the Construction of Radiometallated Bioconjugates for Positron Emission Tomography. *Dalt. Trans.* **2011**, *40* (23), 6168–6195. https://doi.org/10.1039/c0dt01595d.

(4) Fay, R.; Holland, J. P. The Impact of Emerging Bioconjugation Chemistries on Radiopharmaceuticals. *J. Nucl. Med.* **2019**, *60* (5), 587–591. https://doi.org/10.2967/jnumed.118.220806.

(5) S. Lewis, J.; Windhorst, A.; Zeglis, B. *Radiopharmaceutical Chemistry*; Springer, Berlin, Heidelberg, 2019. https://doi.org/10.1007/978-3-319-98947-1.

(6) Othman, M. F. bi.; Mitry, N. R.; Lewington, V. J.; Blower, P. J.; Terry, S. Y. A. Re-Assessing Gallium-67 as a Therapeutic Radionuclide. *Nucl. Med. Biol.* **2017**, *46*, 12–18. https://doi.org/10.1016/j.nucmedbio.2016.10.008.

(7) Poot, A. J.; Adamzek, K. W. A.; Windhorst, A. D.; Vosjan, M. J. W. D.; Kropf, S.; Wester, H.-J.; van Dongen, G. A. M. S.; Vugts, D. J. Fully Automated 89 Zr Labeling and Purification of Antibodies. *J. Nucl. Med.* **2019**, *60* (6), 691–695. https://doi.org/10.2967/jnumed.118.217158.

(8) Marlow, F. L.; Liu, Y.; Wu, P.; Besanceney-Webler, C.; Jiang, H.; Zheng, T.; Feng, L.; Soriano Del Amo, D.; Wang, W.; Klivansky, L. M. Increasing the Efficacy of Bioorthogonal Click Reactions for Bioconjugation: A Comparative Study. *Angew. Chemie - Int. Ed.* **2011**, *50* (35), 8051–8056. https://doi.org/10.1002/anie.201101817.

(9) Klán, P.; Wirz, J. *Photochemistry of Organic Compounds: From Concepts to Practice*; John Wiley & Sons, Ltd, 2009. https://doi.org/10.1002/9781444300017.

(10) Chowdhry, V.; Westheimer, F. H. Photoaffinity Labeling of Biological Systems. *Annu. Rev. Biochem.* **1979**, *48* (1), 293–325. https://doi.org/10.1146/annurev.bi.48.070179.001453.

(11) William B. Jakoby, M. W. *Affinity Labeling*; Elsevier Inc., 1977; Vol. 46. https://doi.org/10.1016/s0076-6879(77)46012-9.

(12) Hashizume, K.; Hashimoto, N.; Miyake, Y. Synthesis of Positron Labeled Photoactive Compounds: 18F Labeled Aryl Azides for Positron Labeling of Biochemical Molecules. *J. Org. Chem.* **1995**, *60* (21), 6680–6681. https://doi.org/10.1021/jo00126a015.

(13) Sykes, T. R.; Woo, T. K.; Baum, R. P.; Qi, P.; Noujaim, A. Direct Labeling of Monoclonal Antibodies with Technetium-99m by Photoactivation. *J. Nucl. Med.* **1995**, *36*

(10), 1913–1922.

(14) Wester, H. J.; Hamacher, K.; Stöcklin, G. A Comparative Study of N.C.A. Fluorine-18 Labeling of Proteins via Acylation and Photochemical Conjugation. *Nucl. Med. Biol.* **1996**, *23* (3), 365–372. https://doi.org/10.1016/0969-8051(96)00017-0.

(15) Pandurangi, R. S.; Karra, S. R.; Katti, K. V.; Kuntz, R. R.; Volkert, W. A. Chemistry of Bifunctional Photoprobes. 1. Perfluoroaryl Azido Functionalized Phosphorus Hydrazides as Novel Photoreactive Heterobifunctional Chelating Agents: High Efficiency Nitrene Insertion on Model Solvents and Proteins. *J. Org. Chem.* **1997**, *62* (9), 2798–2807. https://doi.org/10.1021/jo961867b.

(16) Lange, C. W.; VanBrocklin, H. F.; Taylor, S. E. Photoconjugation of 3-Azido-5-Nitrobenzyl-[18F]Fluoride to an Oligonucleotide Aptamer. *J. Label. Compd. Radiopharm.* **2002**, *45* (3), 257–268. https://doi.org/10.1002/jlcr.565.

(17) Pandurangi, R. S.; Lusiak, P.; Kuntz, R. R.; Volkert, W. A.; Rogowski, J.; Platz, M. S. Chemistry of Bifunctional Photoprobes. 3. Correlation between the Efficiency of CH Insertion by Photolabile Chelating Agents and Lifetimes of Singlet Nitrenes by Flash Photolysis: First Example of Photochemical Attachment of 99mTc-Complex with Human Serum. *J. Org. Chem.* **1998**, *63* (24), 9019–9030. https://doi.org/10.1021/jo981458a.

(18) Patra, M.; Eichenberger, L. S.; Fischer, G.; Holland, J. P. Frontispiece: Photochemical Conjugation and One-Pot Radiolabelling of Antibodies for Immuno-PET. *Angew. Chemie Int. Ed.* **2019**, *58* (7), 1928–1933. https://doi.org/10.1002/anie.201980761.

(19) Eichenberger, L. S.; Patra, M.; Holland, J. P. Photoactive Chelates for Radiolabelling Proteins. *Chem. Commun.* **2019**, *55*, 2257–2260. https://doi.org/10.1039/c8cc09660k.

(20) Patra, M.; Klingler, S.; Eichenberger, L. S.; Holland, J. Simultaneous Photoradiochemical Labelling of Antibodies for Immuno-PET. *SSRN Electron. J.* **2019**, *13*, 416–441. https://doi.org/10.2139/ssrn.3307531.

(21) Fay, R.; Gut, M.; Holland, J. P. Photoradiosynthesis of 68Ga-Labeled HBED-CC-Azepin-MetMAb for Immuno-PET of c-MET Receptors. *Bioconjug. Chem.* **2019**, *30* (6), 1814–180. https://doi.org/10.1021/acs.bioconjchem.9b00342.

(22) Deblonde, G. J. P.; Kelley, M. P.; Su, J.; Batista, E. R.; Yang, P.; Booth, C. H.; Abergel, R. J. Spectroscopic and Computational Characterization of Diethylenetriaminepentaacetic Acid/Transplutonium Chelates: Evidencing Heterogeneity in the Heavy Actinide(III) Series. *Angew. Chemie - Int. Ed.* **2018**, *57*, 4521–4526. https://doi.org/10.1002/anie.201709183.

(23) Ma, C.; Li, Y.; Wang, J.; Qin, C.; Kong, D.; Gao, J.; Wu, Q. Syntheses and Structural Determination of Binuclear Nine-Coordinate (NH 4) 4 [Sm III2 (Httha) 2]·16H 2 O and 2-D Ladder-like Binuclear Nine-Coordinate (NH 4) 4 [Sm III2 (Dtpa) 2]·10H 2 O. *J. Coord. Chem.* **2014**, *67* (4), 597–610. https://doi.org/10.1080/00958972.2014.892074.

(24) Wadas, T. J.; Wong, E. H.; Weisman, G. R.; Anderson, C. J. Coordinating Radiometals of

Copper, Gallium, Indium, Yttrium, and Zirconium for PET and SPECT Imaging of Disease. *Chem. Rev.* **2010**, *110* (5), 2858–2902.

(25) Wagner, M.; Ruloff, R.; Hoyer, E.; Gründer, W. New Gadolinium Complexes as Magnetic Resonance Imaging - Contrast Agents. *Zeitschrift fur Naturforsch. Sect. C - J. Biosci.* **1997**, *52* (7–8), 508–515.

(26) Nishikawa, M.; Nakano, T.; Okabe, T.; Hamaguchi, N.; Yamasaki, Y.; Takakura, Y.; Yamashita, F.; Hashida, M. Residualizing Indium-111-Radiolabel for Plasmid DNA and Its Application to Tissue Distribution Study. *Bioconjug. Chem.* **2003**, *14* (5), 955–961. https://doi.org/10.1021/bc034032y.

(27) Krenning, E. P.; Kwekkeboom, D. J.; Bakker, W. H.; Breeman, W. A. P.; Kooij, P. P. M.; Oei, H. Y.; van Hagen, M.; Postema, P. T. E.; de Jong, M.; Reubi, J. C.; Visser, T. J.; Reijs A. E.M.; Hofland, L.J.; Koper, J. W.; Lamberts, S. W.J. Somatostatin Receptor Scintigraphy with [111In-DTPA-d-Phe1]- and [123I-Tyr3]-Octreotide: The Rotterdam Experience with More than 1000 Patients. *Eur. J. Nucl. Med.* **1993**, *20* (8), 716–731. https://doi.org/10.1007/BF00181765.

(28) Tofts, P. S. Modeling Tracer Kinetics in Dynamic Gd-DTPA MR Imaging. *J. Magn. Reson. Imaging* **1997**, *7* (1), 91–101. https://doi.org/10.1002/jmri.1880070113.

(29) Weinmann, H. J.; Brasch, R. C.; Press, W. R.; Wesbey, G. E. Characteristics of Gadolinium-DTPA Complex: A Potential NMR Contrast Agent. *Am. J. Roentgenol.* **1984**, *142* (3), 619–624. https://doi.org/10.2214/ajr.142.3.619.

(30) Pfeifer, A.; Knigge, U.; Binderup, T.; Mortensen, J.; Oturai, P.; Loft, A.; Berthelsen, A. K.; Langer, S. W.; Rasmussen, P.; Elema, D.; von Benzon, E.; Hojgeerd, L.; Kjaer, A. 64Cu-DOTATATE PET for Neuroendocrine Tumors: A Prospective Head-to-Head Comparison with 111In-DTPA-Octreotide in 112 Patients. *J. Nucl. Med.* **2015**, *56* (8), 847–854. https://doi.org/10.2967/jnumed.115.156539.

(31) Caravan, P.; Ellison, J. J.; McMurry, T. J.; Lauffer, R. B. Gadolinium(III) Chelates as MRI Contrast Agents: Structure, Dynamics, and Applications. *Chem. Rev.* **1999**, *99* (9), 2293–2352. https://doi.org/10.1021/cr980440x.

(32) Byegård, J.; Skarnemark, G.; Skålberg, M. The Stability of Some Metal EDTA, DTPA and DOTA Complexes: Application as Tracers in Groundwater Studies. *J. Radioanal. Nucl. Chem.* **1999**, *241* (2), 281–290. https://doi.org/10.1007/BF02347463.

(33) Corman, M. L.; Galandiuk, S.; Block, G. E.; Prager, E. D.; Weiner, G. J.; Kahn, D.; Abdel-Nabi, H.; Mitchell, E. P.; Pascucci, V. L.; Maroli, A. N.; Maguire, R. T. Immunoscintigraphy With111 In-Satumomab Pendetide in Patients with Colorectal Adenocarcinoma: Performance and Impact on Clinical Management. *Dis. Colon Rectum* **1994**, *37* (2), 129–137. https://doi.org/10.1007/BF02047534.

(34) Boros, E.; Holland, J. P. Chemical Aspects of Metal Ion Chelation in the Synthesis and Application Antibody-Based Radiotracers. *J. Label. Compd. Radiopharm.* **2018**, *61* (9), 652–671. https://doi.org/10.1002/jlcr.3590.

(35) Walsh, G. Biopharmaceutical Benchmarks 2010. *Nat. Biotechnol.* **2010**, *28* (9), 917.

(36) Manyak, M. J.; Hinkle, G. H.; Olsen, J. O.; Chiaccherini, R. P.; Partin, A. W.; Piantadosi, S.; Burgers, J. K.; Texter, J. H.; Neal, C. E.; Libertino, J. A.; Wright, G. L.; Maguire. R. T. Immunoscintigraphy with Indium-111-Capromab Pendetide: Evaluation before Definitive Therapy in Patients with Prostate Cancer. *Urology* **1999**, *54* (6), 1058–1063. https://doi.org/10.1016/s0090-4295(99)00314-3.

(37) Gritsan, N. P.; Platz, M. S. Kinetics, Spectroscopy, and Computational Chemistry of Arylnitrenes. *Chem. Rev.* **2006**, *106* (9), 3844–3867. https://doi.org/10.1021/cr040055+.

(38) Holland, J. P. Chemical Kinetics of Radiolabelling Reactions. *Chem. - A Eur. J.* **2018**, *24* (62), 16472–16483. https://doi.org/10.1002/chem.201803261.

Graphical abstract

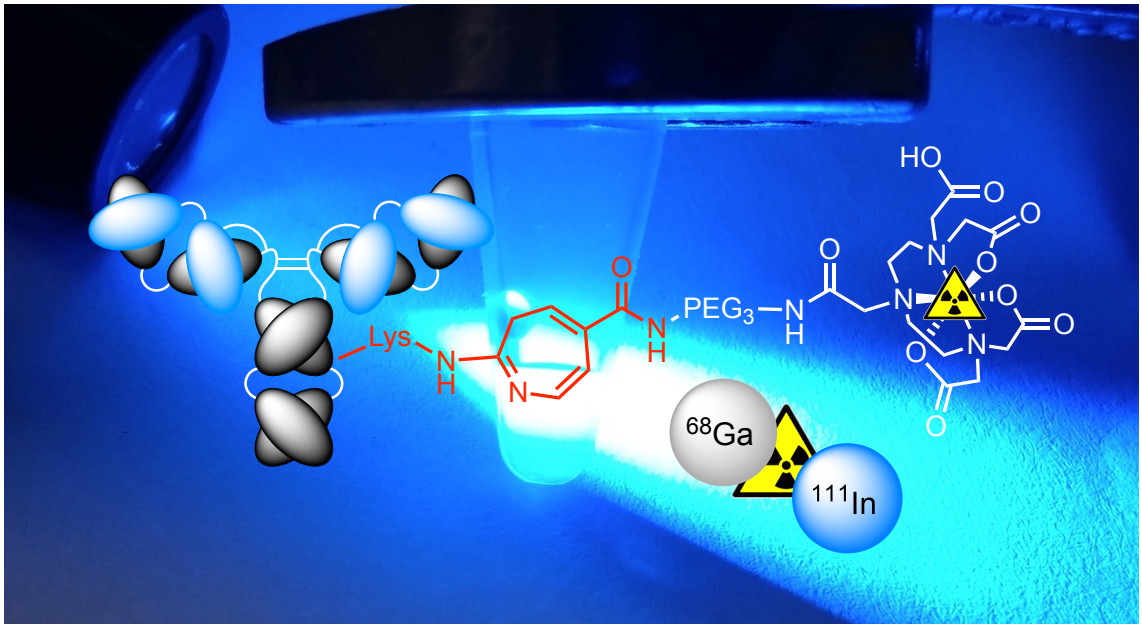

Synopsis

Photoradiosynthesis was used to functionalise proteins with chelates for imaging and therapy. The DTPA-PEG_3-ArN_3 ligand and the corresponding Ga^{3+} and In^{3+} complexes were synthesised and photoactivation experiments with ultraviolet light (365 nm) showed fast reaction kinetics. Photochemically induced bioconjugation reactions between ^{68}Ga- or ^{111}In-radiolabelled DTPA-PEG_3-ArN_3 and trastuzumab showed conversions between 4 and 12%. The use of DTPA expands the scope of photochemical conjugation methods to include metal ions like In^{3+} and potentially lanthanides.